Directed self-avoiding walks on Sierpinski carpets: series results

1995 J. Phys. A: Math. Gen. 28 1257

(http://iopscience.iop.org/0305-4470/28/5/014)

J. Phys. A: Math. Gen. 28 (1995) 1257–1270. Printed in the UK

Directed self-avoiding walks on Sierpinski carpets: series results

F D A Aarão Reis and R Riera

Departamento de Física Pontifícia Universidade Católica do Rio de Janeiro C P 38071, 22452-970 Rio de Janeiro RJ, Brazil

Received 29 April 1994, in final form 9 August 1994

Abstract. Using a graph counting technique suitable for self-similar fractals we obtain the exact densities of partially (PDSAW) and fully (FDSAW) directed self-avoiding walks on Sierpinski carpets. From them we calculate the root-mean-square transverse and longitudinal displacements of the n-step walks up to $n = 20$ for PDSAWs and up to $n = 23$ for FDSAWs.

The critical exponents $\nu_\perp$ found for the PDSAW depend on the fractal dimension as well as on the lacunarity of the lattice. The results indicate that PDSAWs and FDSAWs have different critical behaviour on the same carpet.

1. Introduction

It has been realized that the introduction of a global bias in geometrical models such as percolation or self-avoiding walks (SAWs) leads to novel anisotropic critical behaviour (see [1] and references therein).

Here, we study the directed SAW models (DSAWs) which are self-avoiding walk models restricted not to step in several particular directions.

The introduction of a preferred direction gives rise to two independent correlation lengths, parallel and perpendicular to the preferred direction. They are given respectively by the root-mean-square longitudinal displacement $\langle R^2_{\parallel n}\rangle^{1/2}$ and by the root-mean-square perpendicular displacement $\langle R^2_{\perp n}\rangle^{1/2}$ of the walk. They vary with the number of steps n as

$$\langle R^2_{\parallel n}\rangle^{1/2} \sim n^{\nu_\parallel} \tag{1a}$$

$$\langle R^2_{\perp n}\rangle^{1/2} \sim n^{\nu_\perp}. \tag{1b}$$

Figure 1 shows two types of DSAWs on a square lattice. The partially directed SAW model (PDSAW) is a three-choice model for which the steps upward, downward or to the right are allowed. The fully directed SAW (FDSAW) is a two-choice model for which only steps upward and to the right are allowed. The corresponding longitudinal and perpendicular directions are also shown in figure 1.

Nadal *et al* [2] have pointed out that any fully directed SAW can be decomposed into a forward walk along the preferred direction and a random walk perpendicular to this direction. Later, Redner and Majid [3], Szpilka [4] and Blöte and Hilhorst [5], using several techniques, obtained the exact results $\gamma = 1$, $\nu_\parallel = 1$ and $\nu_\perp = \frac{1}{2}$ for DSAWs on Euclidean lattices. Their results are valid for general dimensions $E \geqslant 2$, regardless of the detailed restrictions of the steps and include the PDSAW and FDSAW models defined above for the square lattice.

0305-4470/95/051257+14$19.50

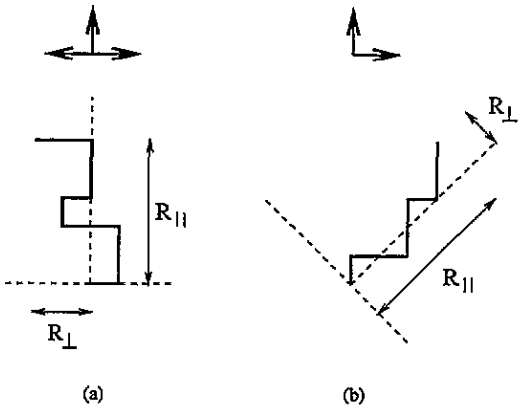

Figure 1. Illustration of (a) PDSAW, (b) FDSAW on the square lattice. Also shown are the longitudinal ($R_\parallel$) and transverse ($R_\perp$) displacement of each walk. The arrows indicate the allowed directions of the steps.

In fact, from a field-theoretic approach, Cardy [6] has shown that directed SAWs are in the same universality class as directed random walks, and therefore should exhibit mean-field exponents $\gamma = 1$, $\nu_\parallel = 1$ and $\nu_\perp = \frac{1}{2}$ in all dimensions.

The results of Zhang *et al* [7] from an exact enumeration up to $n = 10$ of five-choice partially directed self-avoiding walks on the cubic lattice also support that various partially directed SAWs belong to the same universality class as fully directed SAWs and that the asymptotic behaviour is dimension independent for $E \geqslant 2$.

The question of universality classes of DSAWs on fractals then naturally arises. Some non-trivial versions of directed walks were proposed which are exact soluble on the Sierpinski gasket type of fractals, as for instance the piecewise directed random walks, for which the allowed directions depend on the site they visit [8, 9]. For these walks, it was obtained that the critical exponent ν associated with the mean squared end-to-end distance of n-step walks ($\langle R_n^2 \rangle \sim n^{2\nu}$) is model dependent for each gasket.

Recently, DSAWs were studied on a family of infinitely ramified fractals, the Sierpinski carpets [10], but still there is some controversy about their critical behaviour. Yao and Zhang [11] and Yao *et al* [12] analysed PDSAWs and FDSAWs respectively on some carpets at finite stages of their constructions through Monte Carlo simulations. They obtained $0.5 < \nu_\perp < 1.0$ and the dimension independent value $\nu_\parallel = 1$. Their estimates support the hypothesis that PDSAWs and FDSAWs have the same asymptotic behaviour on each carpet. On the other hand, Kim *et al* [13] argued that $\nu_\perp = 1$ for all carpets based on analytic arguments and simulations.

In this work, we study PDSAWs and FDSAWs on the Sierpinski carpets through series expansion techniques [14]. We apply a graph counting method that gives the density of connected graphs (number of embeddings per number of sites) in the limit of the infinite fractal lattice.

The paper is organized as follows. In section 2 we show the graph counting method. In section 3 we present the series analysis method used here and the results. In section 4 we give arguments based on the geometrical properties of the carpets to analyse our estimates and compare them with previous results in the literature.

2. Series expansions for Sterpinski carpets

The Sierpinski carpets are constructed by the recursive iteration of a generator (in figure 2 we show the generators of carpets numbered as 1 to 6 respectively). These generators are

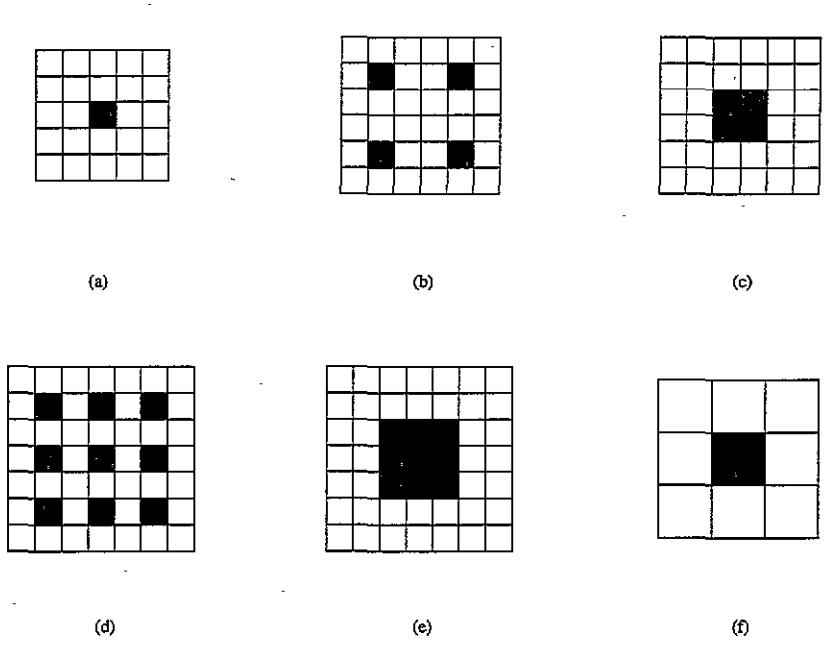

Figure 2. Generators of Sierpinski carpets (a) $b = 5$, $m = 1$; (b) and (c) $b = 6$, $m = 4$; (d) and (e) $b = 7$, $m = 9$; (f) $b = 3$, $m = 1$.

formed by an initial square divided in b^2 subsquares from which m are eliminated according to a fixed rule. This procedure is repeated indefinitely for the remaining squares to construct the fractal lattice, whose sites are located at the corners of the non-eliminated squares. The fractal dimension of the lattice is [10]:

$$D_F = \frac{\ln(b^2 - m)}{\ln b}. \tag{2}$$

A graph counting method [14] is used to find the number of embeddings of a graph in any stage of the construction of the carpet. This technique has already been applied to the SAW, to the Ising model and to ideal chains on these lattices [15–17].

In figure 3 we show two possible embeddings of a graph (a PDSAW with three steps) in the second stage of carpet 2. Due to the self-similar constructing process, the lattice at the $(\ell + 1)$th stage is obtained by the reproduction of ℓth stage structure in the non-eliminated squares of the generator. As a consequence, the number of embeddings $G(\ell)$ of a graph in any stage ℓ can be obtained from the number of embeddings $G(\ell_0)$ of the graph in a small stage ℓ_0 as well as from the number of embeddings that cross two, three or four adjacent stages ℓ_0 (the stage ℓ_0 is the minimal stage in which the graph can be embedded). It was shown that [14]:

$$G(\ell) = A(b^2 - m)^\ell + Bb^\ell + C \tag{3}$$

where A, B and C are rational constants.

The number of sites $N(\ell)$ belonging to the carpet at the ℓth stage of construction also behaves as (3), with constants A', B' and C' [14]:

$$N(\ell) = A'(b^2 - m)^\ell + B'b^\ell + C'. \tag{4}$$

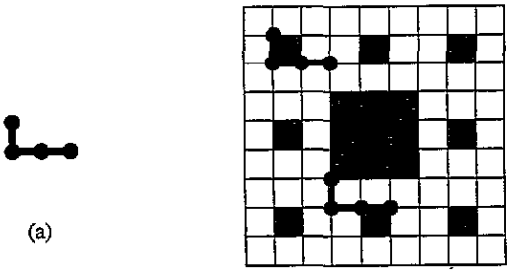

(a) (b)

Figure 3. A particular PDSAW with three steps (a) and two possible embeddings on carpet 6 at the second stage of construction (b).

The density of the graph in the fractal is then:

$$\rho = \lim_{\ell \to \infty} \frac{G(\ell)}{N(\ell)} = \frac{A}{A'}. \tag{5}$$

After the enumeration of PDSAWs and FDSAWs in the square lattice, the density of each walk can be calculated according to (3), (4) and (5). From these densities we obtained $\langle R^2_{\perp n} \rangle$ nd $\langle R^2_{\parallel n} \rangle$ *for n-step* PDSAWs *on carpets 1–6 up to order* $n = 20$ *and* $\langle R^2_{\perp n} \rangle$ *for n-step* FDSAWs on the same carpets up to order $n = 23$. The lengths are measured as in the square lattice (see figure 1). The results are shown in tables 1–3 respectively.

3. Series analysis and results

In order to find $\nu_\perp$ one should consider the $\langle R^2_{\perp n} \rangle$ generating function

$$R_\perp(x) = \sum_{n=1}^{\infty} \langle R^2_{\perp n} \rangle x^n \tag{6}$$

which behaves as $(x_c - x)^{-(2\nu_\perp + 1)}$ near the biased critical point $x_c = 1$, in analogy with the mean squared end-to-end distance ($\langle R^2_n \rangle$) generating function for SAWs [18].

First, we consider the most used methods for series analysis, the Padé approximants and its generalizations [18, 19]. These methods however are not suitable for PDSAW and FDSAW series. In fact, series (6) for PDSAWs and FDSAWs on the square lattice are rational fractions [3] and after a certain order the approximants become indeterminate [20]. On carpets, many approximants are defective (specially for FDSAWs), suggesting that the method is not appropriate as well.

Another series analysis technique is the ratio method. According to this method, the critical point and the critical exponent of the generating function are obtained from the ratio between two consecutive series coefficients. From (1*b*) and (6) it is expected that

$$\mu'_n = \frac{\langle R^2_{\perp n} \rangle}{\langle R^2_{\perp n-1} \rangle} \approx 1 + 2\nu_\perp \frac{1}{n} \qquad (n \to \infty). \tag{7}$$

Plotting μ'_n versus $1/n$ one obtains estimates of $\nu_\perp$ from the slope of the plot. More precisely, we calculate

$$\nu'_{\perp n} = \frac{n}{2}(\mu'_n - 1) \tag{8}$$

Table 1. Root-mean-square transverse displacement $(R^2_{\perp n})^{1/2}$ according to the number of steps n of PDSAWS on carpets 1–6 (see text).

n	carpet 1	carpet 2	carpet 3	carpet 4	carpet 5	carpet 6
2	2.57142857142857E+0000	2.57142857142857E+0000	2.57142857142857E+0000	2.57142857142857E+0000	2.57142857142857E+0000	2.57142857142857E+0000
3	4.23176030774232E+0000	4.22593728360867E+0000	4.22904368358814E+0000	4.22018032306446E+0000	4.21483375959079E+0000	4.21734104046243E+0000
4	5.99109981791994E+0000	5.97584493874020E+0000	5.98676047329709E+0000	5.96020873621588E+0000	5.95793431717148E+0000	5.95515619751428E+0000
5	7.77070437021883E+0000	7.74035456057371E+0000	7.76512485713296E+0000	7.70829781995189E+0000	7.71120588263951E+0000	7.70434273481598E+0000
6	9.56239609465905E+0000	9.51210773289184E+0000	9.56514296563737E+0000	9.45731267378798E+0000	9.49013741189487E+0000	9.46367905316371E+0000
7	1.13570400275622E+0001	1.12821454665454E+0001	1.13623169019448E+0001	1.11978395181389E+0001	1.12768410221203E+0001	1.12207063845965E+0001
8	1.31524932451945E+0001	1.30479995736310E+0001	1.31449884402229E+0001	1.29279632072331E+0001	1.30383492689319E+0001	1.29754086122419E+0001
9	1.49475162843635E+0001	1.48076524859214E+0001	1.49207755489885E+0001	1.46482271288300E+0001	1.47634010552730E+0001	1.47200363864028E+0001
10	1.67419262644325E+0001	1.65592836388254E+0001	1.66583482978474E+0001	1.63610441883930E+0001	1.64257749862230E+0001	1.64484811808839E+0001
11	1.85355121010456E+0001	1.83028356465811E+0001	1.83856555749917E+0001	1.80668362712705E+0001	1.80085582562557E+0001	1.81666087886922E+0001
12	2.03283564657154E+0001	2.00384334261097E+0001	2.01150598713999E+0001	1.97628974159527E+0001	1.95445034868221E+0001	1.98706308262720E+0001
13	2.21204369741557E+0001	2.17673094125541E+0001	2.18481867973730E+0001	2.14411365750428E+0001	2.10845303734678E+0001	2.15607417473318E+0001
14	2.39118366121794E+0001	2.34909862139032E+0001	2.35932761969509E+0001	2.30930591843715E+0001	2.26390740009605E+0001	2.32282799768295E+0001
15	2.57025700413527E+0001	2.52116406865527E+0001	2.53396905368098E+0001	2.47071655280034E+0001	2.42194928249258E+0001	2.48662366059048E+0001
16	2.74926488682927E+0001	2.69301263004265E+0001	2.70846056706597E+0001	2.62788454306209E+0001	2.58239529991837E+0001	2.64862364390518E+0001
17	2.92820150814005E+0001	2.86468866680420E+0001	2.88238133497810E+0001	2.78005708247653E+0001	2.74341172175457E+0001	2.81018986336404E+0001
18	3.10705810525712E+0001	3.03604681510196E+0001	3.05791736150788E+0001	2.92757485962403E+0001	2.90454240756078E+0001	2.97183115314002E+0001
19	3.28582466133260E+0001	3.20683595713458E+0001	3.23279332420434E+0001	3.07048589538329E+0001	3.06617361607121E+0001	3.13442578600377E+0001
20	2.46449517162739E+0001	3.37574996365115E+0001	3.40739618515521E+0001	3.20967218338049E+0001	3.23023774205892E+0001	3.29813698966772E+0001

Table 2. Root-mean-square longitudinal displacement $\langle R^2_{\|n} \rangle^{1/2}$ according to the number steps n of PDSAWs on carpets 1–6 (see text).

n	carpet 1	carpet 2	carpet 3	carpet 4	carpet 5	carpet 6
2	3.42857142857143E+0000	3.42857142857143E+0000	3.42857142857143E+0000	3.42857142857143E+0000	3.42857142857143E+0000	3.42857142857143E+0000
3	7.23176030774232E+0000	7.22593728360866E+0000	7.22904368358914E+0000	7.22018032306446E+0000	7.21483375959079E+0000	7.21734104046243E+0000
4	1.25781177813409E+0001	1.25659066171751E+0001	1.25732811000959E+0001	1.25535347869090E+0001	1.25439488923961E+0001	1.25471951629157E+0001
5	1.94099315936154E+0001	1.93857232162867E+0001	1.94073390364701E+0001	1.93608917173324E+0001	1.93480171980631E+0001	1.93470894436872E+0001
6	2.77412601102956E+0001	2.76994160562102E+0001	2.77532875605149E+0001	2.76556883557664E+0001	2.76653190554044E+0001	2.76474520232876E+0001
7	3.75685488880449E+0001	3.75018044413612E+0001	3.76070253412981E+0001	3.74308221647292E+0001	3.75045967119068E+0001	3.74565010018712E+0001
8	4.88921333627107E+0001	4.87931347903017E+0001	4.90186937141561E+0001	4.86837686294139E+0001	4.89403855547138E+0001	4.87891152524194E+0001
9	6.17116287339386E+0001	6.15740259274615E+0001	6.19434413274466E+0001	6.14110349070333E+0001	6.19972861482373E+0001	6.16427172774503E+0001
10	7.60270989734544E+0001	7.58487348847572E+0001	7.64372201635419E+0001	7.56141049193417E+0001	7.66993185408035E+0001	7.60248004125694E+0001
11	9.18381750646706E+0001	9.16218862229291E+0001	9.24421009614857E+0001	9.13102079935485E+0001	9.30517275360991E+0001	9.19387381027840E+0001
12	1.09144963896182E+0002	1.08897292892243E+0002	1.09961011361939E+0002	1.08531376027321E+0002	1.11018595877412E+0002	1.09390619730909E+0002
13	1.27947175225677E+0002	1.27677046140340E+0002	1.28986019751032E+0002	1.27325258861532E+0002	1.30570601949109E+0002	1.28382774019769E+0002
14	1.48244957586723E+0002	1.47959084126373E+0002	1.49423856620885E+0002	1.47729343151336E+0002	1.51609084596057E+0002	1.48913801104026E+0002
15	1.70038500868301E+0002	1.69739564190856E+0002	1.71383488880390E+0002	1.69769817570323E+0002	1.74065205049011E+0002	1.70981195358976E+0002
16	1.93328584939000E+0002	1.93013166932891E+0002	1.94752705669478E+0002	1.93448045090963E+0002	1.97917886738885E+0002	1.94573456459596E+0002
17	2.18116354852751E+0002	2.17777350703735E+0002	2.19661977300777E+0002	2.18751566202114E+0002	2.23144963788367E+0002	2.19681711825259E+0002
18	2.44403294000269E+0002	2.44036127554439E+0002	2.46057618418592E+0002	2.45659622241611E+0002	2.49783008540584E+0002	2.46275828635956E+0002
19	2.72190776444819E+0002	2.71799781619437E+0002	2.73988039022354E+0002	2.74149030515915E+0002	2.77879983938061E+0002	2.74332431541601E+0002
20	3.01479740779429E+0002	3.01096794767683E+0002	3.03514752803302E+0002	3.04201307482928E+0002	3.07483056829918E+0002	3.03835070235766E+0002

Table 3. Root-mean-square transverse displacement $(R^2_{\perp n})^{1/2}$ according to the number of steps n of FDSAWS on carpets 1–6 (see text).

n	carpet 1	carpet 2	carpet 3	carpet 4	carpet 5	carpet 6
2	2.00000000000000E+0000	2.00000000000000E+0000	2.00000000000000E+0000	2.00000000000000E+0000	2.00000000000000E+0000	2.00000000000000E+0000
3	3.00000000000000E+0000	3.00000000000000E+0000	3.00000000000000E+0000	3.00000000000000E+0000	3.00000000000000E+0000	3.00000000000000E+0000
4	4.00000000000000E+0000	4.00000000000000E+0000	4.00764315506154E+0000	4.00000000000000E+0000	4.01521505900712E+0000	4.00000000000000E+0000
5	5.00000000000000E+0000	5.00000000000000E+0000	5.02135170038743E+0000	5.00000000000000E+0000	5.04223396358238E+0000	5.01607163356676E+0000
6	6.00000000000000E+0000	6.00000000000000E+0000	6.06427331936087E+0000	6.00000000000000E+0000	6.12414026225229E+0000	6.05321251558367E+0000
7	7.00000000000000E+0000	7.00000000000000E+0000	7.10493491767263E+0000	7.00000000000000E+0000	7.24908609860037E+0000	7.10244672963476E+0000
8	8.00000000000000E+0000	8.00134119612135E+0000	8.13602412232135E+0000	8.00000000000000E+0000	8.37152420921378E+0000	8.16047832585949E+0000
9	9.00000000000000E+0000	9.00493857895066E+0000	9.15877981755801E+0000	9.00859389015916E+0000	9.48741331841404E+0000	9.22906116088820E+0000
10	1.00000000000000E+0001	1.00104914910316E+0001	1.01771276729880E+0001	1.00415461437886E+0001	1.06008389978543E+0001	1.02801656350546E+0001
11	1.10000000000000E+0001	1.10178169658605E+0001	1.11986084380606E+0001	1.11111343158572E+0001	1.17210500103358E+0001	1.12999279024069E+0001
12	1.20000494932331E+0001	1.20267900349797E+0001	1.21182175910194E+0001	1.22184580836728E+0001	1.27380185890581E+0001	1.22928480005926E+0001
13	1.30003299394978E+0001	1.30368914860987E+0001	1.30407790240569E+0001	1.33547718966685E+0001	1.35464794999396E+0001	1.32702286105560E+0001
14	1.40011861217549E+0001	1.40472404512107E+0001	1.39762569968230E+0001	1.45089028884040E+0001	1.42445610271137E+0001	1.42466290802239E+0001
15	1.50030507404848E+0001	1.50582868805939E+0001	1.49212458087141E+0001	1.56746309432765E+0001	1.49415315931593E+0001	1.52368759776144E+0001
16	1.60062883606334E+0001	1.60733331237715E+0001	1.58662823408475E+0001	1.68465454965727E+0001	1.56443997794918E+0001	1.61894817662621E+0001
17	1.70110378423414E+0001	1.70966104532491E+0001	1.68025778154897E+0001	1.80224703650750E+0001	1.63373246766210E+0001	1.70526600064354E+0001
18	1.80171253171096E+0001	1.81285244835730E+0001	1.78415957011802E+0001	1.91866252925561E+0001	1.69913242464475E+0001	1.78667042699304E+0001
19	1.90240749283598E+0001	1.91641968267236E+0001	1.88784578838530E+0001	2.03248212105117E+0001	1.77619972579561E+0001	1.86886376751069E+0001
20	2.00311991804524E+0001	2.02031839924528E+0001	1.99067410549749E+0001	2.14264696111869E+0001	1.87727110543262E+0001	1.95408864181245E+0001
21	2.10377273371752E+0001	2.12446773130974E+0001	2.09303289368656E+0001	2.24847032730728E+0001	1.98762230404002E+0001	2.04244661354068E+0001
22	2.20429324549673E+0001	2.22875210528697E+0001	2.19518167967017E+0001	2.34954922185694E+0001	2.09702228576965E+0001	2.13269512480036E+0001
23	2.30468898532220E+0001	2.33301991597669E+0001	2.29767827429572E+0001	2.44621346086899E+0001	2.20514881283351E+0001	2.22246717225297E+0001

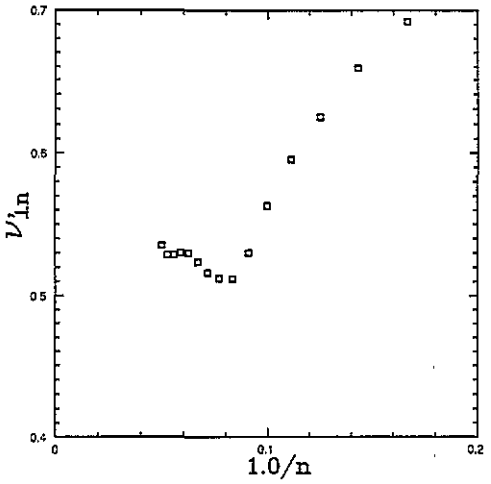

Figure 4. Plot of $\nu'_{\perp n}$ versus $1.0/n$ for a PDSAW on carpet 5.

so that $\nu'_{\perp n} \to \nu$ when $n \to \infty$. However, the ratio method is also not suitable for PDSAWs and FDSAWs on some carpets due to oscillations in $\nu'_{\perp n}$. As an illustration, in figure 4 we plot $\nu'_{\perp n}$ versus $1/n$ for the PDSAW on carpet 5. From this plot, although $\nu'_{\perp n}$ oscillates around 0.5, we cannot get accurate estimates.

Then we propose the root method, based on the root test used to calculate the radius of convergence of series. According to the root test, one should analyse $\lim_{n\to\infty} a_n^{1/n}$ to obtain the convergence properties of the series $\sum_n a_n$. For series (6) we consider

$$\mu_n = \langle R_{\perp n}^2 \rangle^{1/n}. \tag{9}$$

Introducing amplitude $A^{1/2}$ in (1*b*), one has

$$\mu_n \approx A^{1/n} n^{2\nu_\perp/n} \qquad (n \to \infty) \tag{10a}$$

or

$$\mu_n \approx 1 + 2\nu_\perp \frac{\ln n}{n} + \frac{\ln A}{n}. \tag{10b}$$

The third term on the right-hand side of equation (10*b*) does not contribute appreciably if $\ln n \gg |\ln A|$. This condition holds for PDSAWs in the square lattice ($A \approx 1$) when $n \gtrsim 10$. Then:

$$\mu_n \approx 1 + 2\nu_\perp \frac{\ln n}{n}. \tag{10c}$$

From (10*c*) we calculate for each order n the corresponding estimate of $\nu_\perp$:

$$\nu_{\perp n} = \frac{1}{2} \frac{n}{\ln n} (\mu_n - 1). \tag{11}$$

The final estimates of $\nu_\perp$ are obtained by a procedure similar to the construction of Neville tables [18]: we consider $\nu_{\perp n}$, as a function of $\ln n/n$ and find the intercepts at the $\ln n/n = 0$ axis ($n \to \infty$) of straight lines passing through two successive points of the

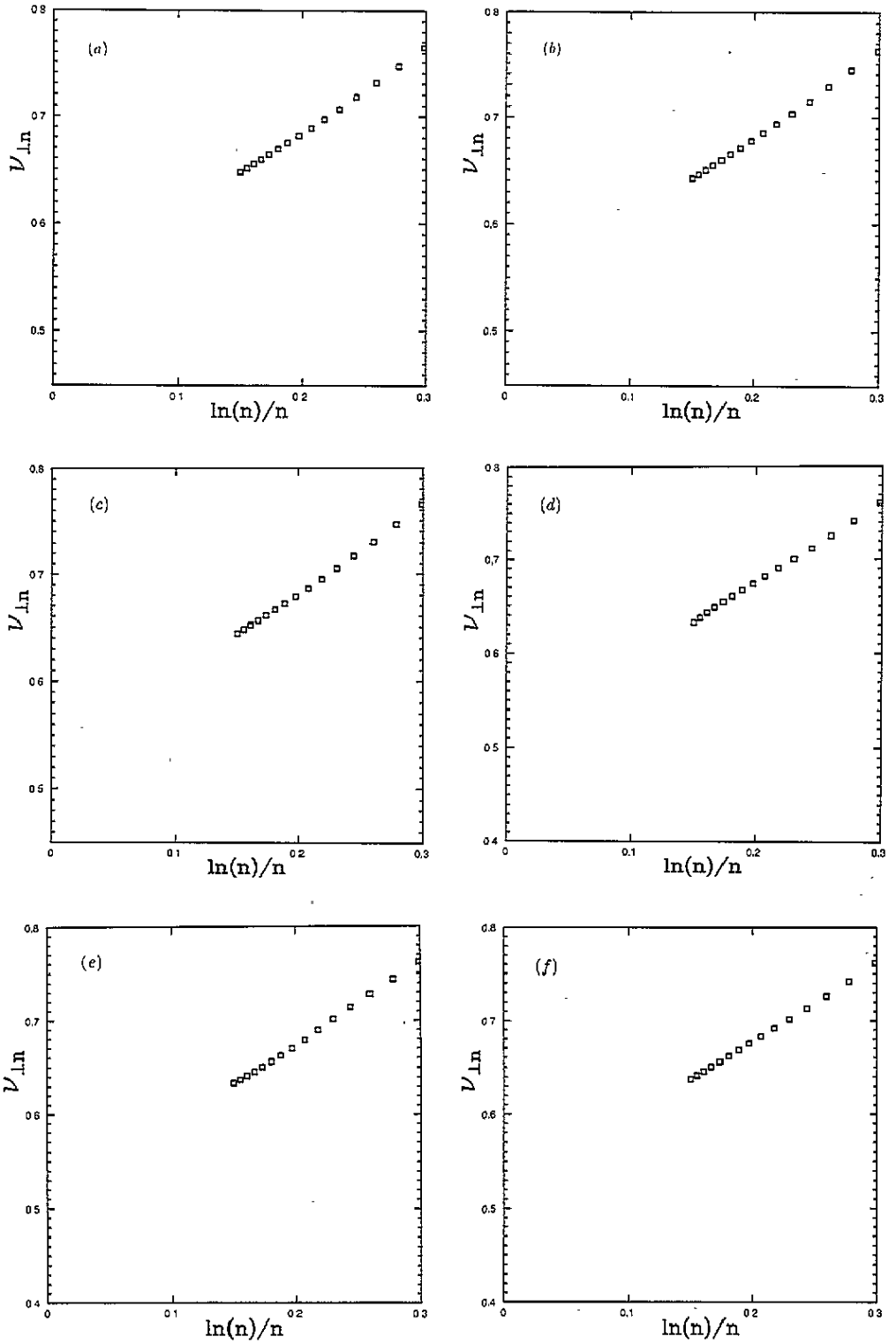

Figure 5. Plot of $\nu_{\perp n}$ versus $\ln n/n$ for PDSAWS on carpets 1–6 ((*a*)–(*f*), respectively).

Table 4. *Final estimates of $\nu_\perp$ for* PDSAWs *on carpets 1–6.*

Carpet	$\nu_\perp$
1	0.55 ± 0.01
2	0.53 ± 0.02
3	0.55 ± 0.02
4	0.46 ± 0.04
5	0.54 ± 0.04
6	0.55 ± 0.05

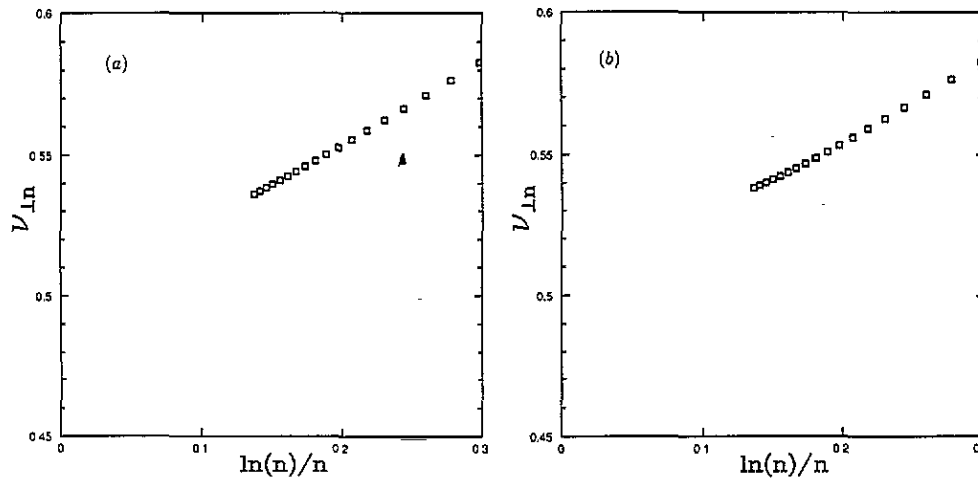

Figure 6. Plot of $\nu_{\perp n}$ versus $\ln n/n$ for FDSAWs (a) on carpet 1 and (b) on carpet 2.

plot. From the convergence of these intercepts we obtain the final estimates. The plots of $\nu_{\perp n}$ versus $\ln n/n$ for PDSAWs on carpets 1–6 are well behaved, as shown in figure 5. In table 4 we show the final estimates of $\nu_\perp$ for PDSAWs on carpets 1–6.

In figure 6 we plot $\nu_{\perp n}$ versus $\ln n/n$ for FDSAWs on carpets 1 and 2. The final estimates $\nu_\perp = 0.50 \pm 0.01$ and $\nu_\perp = 0.51 \pm 0.02$ for carpets 1 and 2 respectively were obtained using the same procedure described above. For carpets 3–6, the plots of $\nu_{\perp n}$ do not show clear convergence properties but the visual inspection of the plots indicates that $0.4 < \nu_\perp < 0.6$.

The slow convergence of series (6) for the FDSAW as compared to the PDSAW can be explained from the relation between their preferred directions and the symmetry axis of the carpets: the longitudinal and perpendicular directions agrees with the direction of the borders of the lacunas in the case of the PDSAW, but not in the case of the FDSAW. Besides, as the FDSAW on the square lattice behaves as $\langle R^2_{\perp n}\rangle = n/2$, the amplitude A for the same model on carpets might contribute to (10b).

In order to find $\nu_\parallel$ in (1a), we consider the $\langle R^2_{\parallel n}\rangle$ generating function

$$R_\parallel(x) = \sum_{n=1}^{\infty} \langle R^2_{\parallel n}\rangle x^n \tag{12}$$

which behaves as $(x_c - x)^{-(2\nu_\parallel + 1)}$ near the biased critical point $x_c = 1$. We also analyse (12) through the root method. Analogously to (11) we calculate the estimate of $\nu_\parallel$ for each

order n from:

$$\nu_{\parallel n} = \frac{1}{2}\frac{n}{\ln n}(\langle R^2_{\parallel n}\rangle^{1/n} - 1). \tag{13}$$

The final estimates of $\nu_\parallel$ are obtained using the same procedure described to get $\nu_\perp$. In figure 7 we plot $\nu_{\parallel n}$ versus $\ln n/n$ for PDSAWs on carpets 1–6. The final estimates of $\nu_\parallel$ are shown in table 5. For FDSAWs all steps contribute to the longitudinal displacement along the forward sense. Then, $\langle R^2_{\parallel n}\rangle^{1/2} \sim n$ leading to the trivial result $\nu_\parallel = 1$.

Table 5. Final estimates of $\nu_\parallel$ for PDSAWs on carpets 1–6.

Carpet	$\nu_\parallel$
1	0.97 ± 0.02
2	0.97 ± 0.03
3	0.97 ± 0.03
4	0.98 ± 0.03
5	0.96 ± 0.03
6	0.97 ± 0.02

4. Conclusions

The estimates of the critical exponents $\nu_\perp$ and $\nu_\parallel$ for the PDSAW and the FDSAW on carpet 1 show that the two models belong to different universality classes, in contrast to the results for Euclidean lattices. This means that the effect of the lacunas on the growth of the walk is different according to the relation between the special directions of the walk (longitudinal and perpendicular) and the directions of the borders of the lacunas.

The lacunarity of the lattice [10] influences the value of $\nu_\perp$. As observed for other models of walks [15, 17], the fractal dimension alone does not define universality classes. According to our results for the PDSAW on carpets 2 and 3 (the lacunarity of carpet 3 is greater than that of carpet 2) and on carpets 4 and 5 (the lacunarity of carpet 5 is greater than that of carpet 4), for carpets with the same D_f, $\nu_\perp$ is larger for lattices with higher lacunarity.

Figure 8 illustrates the influence of the lacunarity on $\nu_\perp$ in the case of PDSAWs. In figure 8(a) the lacuna stretches the walk along the perpendicular direction when it touches the border. This effect is stronger when the lacuna is bigger (high lacunar fractal). On the other hand, in figure 8(b), the lacuna inhibits the growth of the walk along the perpendicular direction. This effect is stronger when the number of lacunas within the lattice is larger (low lacunar fractal).

From the results shown in table 5, the lacunas also inhibit the longitudinal growth of PDSAWs ($\nu_\parallel < 1$).

It is possible to compare the end-to-end distance exponents of DSAWs and SAWs on carpets. For the isotropic SAW, as there is only one length scale, $\nu_\perp = \nu_\parallel = \nu_{SAW}$. From the results reported here for $\nu_\perp$ and $\nu_\parallel$ for DSAWs and the results for ν_{SAW} reported in [15] for SAWs on carpets 1, 4, 5 and 6, $\nu_\perp < \nu_{SAW} < \nu_\parallel$.

Our results also show that $\nu_\perp$ for the PDSAW is different from the exponent ν_{RW} for the random walk problem or ν_{ic} for the ideal chain problem on the same carpet. For fractals, it is expected that ν_{RW} and $\nu_{ic} < \frac{1}{2}$ [21] and here $\nu_\perp > \frac{1}{2}$ for most carpets.

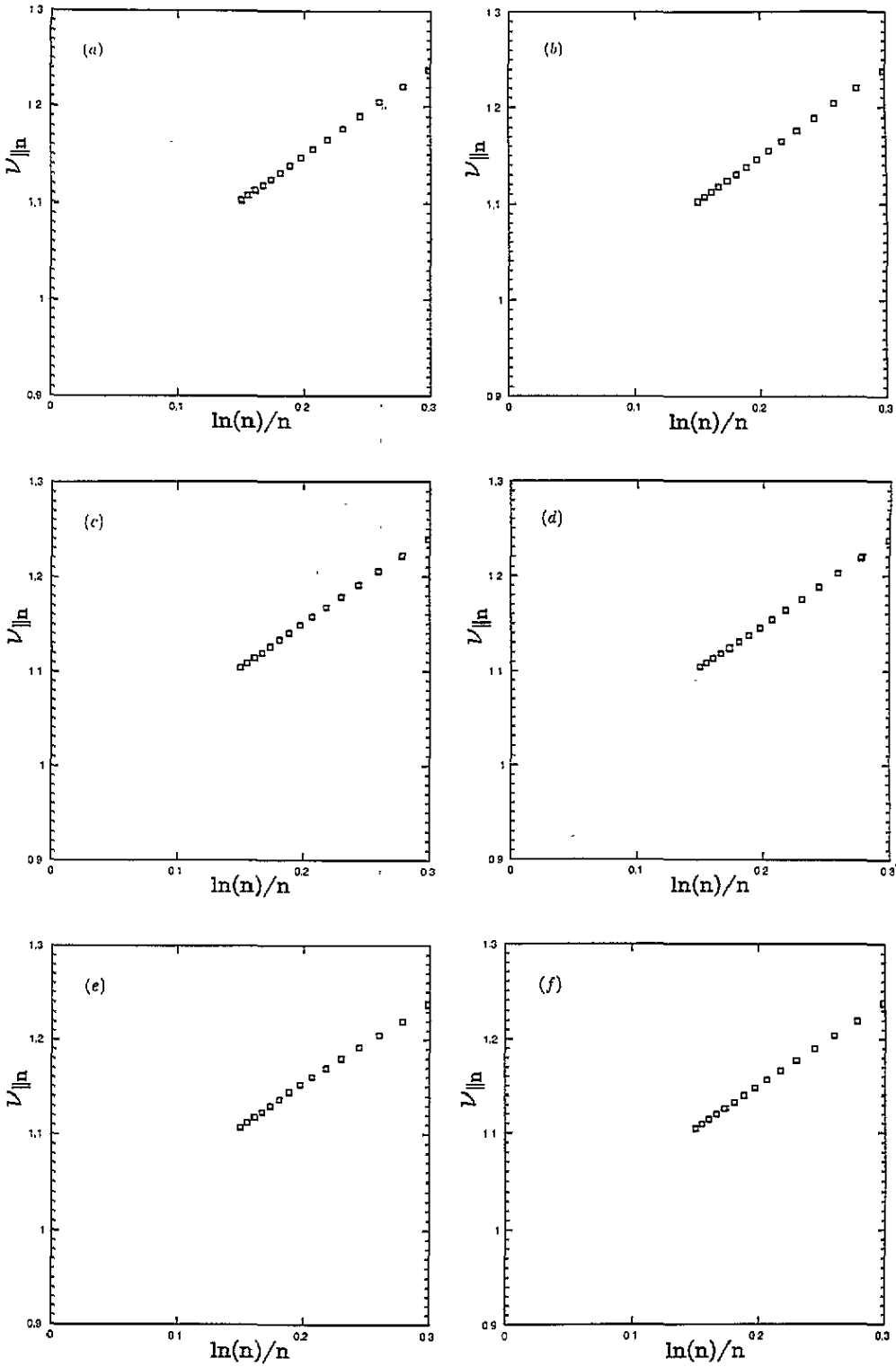

Figure 7. Plot of $\nu_{\|n}$ versus $\ln n/n$ for PDSAWs on carpets 1–6 ((*a*)–(*f*), respectively).

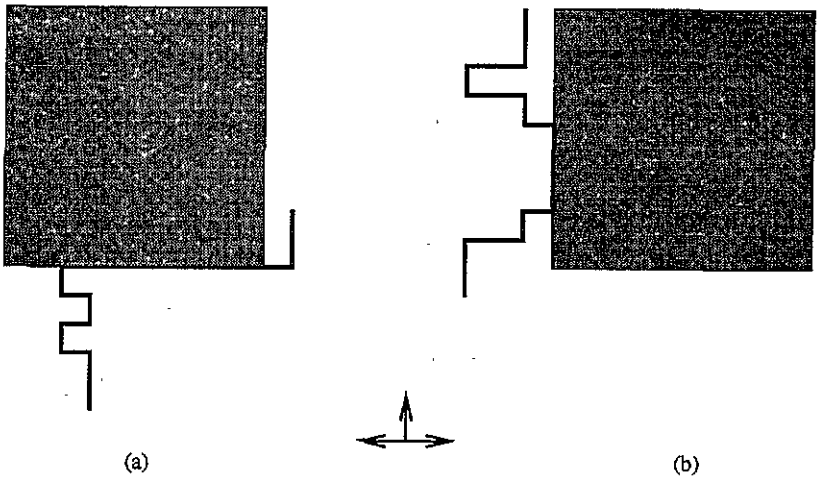

Figure 8. Illustration of the influence of the lacunas on the transverse displacement of a PDSAW; (a) the lacuna stretches the walk, (b) the lacuna compresses the walk. The arrows indicate the allowed directions of the steps.

Our estimates can also be used to test results obtained by other techniques. For instance, the proposal $\nu_\perp = 1$ for FDSAWs of [13] is not tenable. Their arguments are based on a particular ensemble of DSAWs having starting site on the lower left corner of the carpet at a finite-stage of construction. For these walks the probability of not encountering the largest hole is exponentially small [13]. Then, they have overestimated the effect of the larger lacuna in a finite stage of the carpet (this effect is shown in figure 8(a)), overestimating $\nu_\perp$. The same occurs in the simulations reported in [13] in which walks that touch the borders of carpets at the fourth-stage of construction were discarded. As a consequence of this finite-size effect of the lattice, the remainder ensemble of DSAWs used to measure $\langle R^2_{\perp n}\rangle$ were restricted to be embedded in the lattice, enhancing the role of the largest lacuna. On the other hand, our results capture exactly the effect of the distribution of lacunas of all sizes through the infinite fractal lattice because we also include the contribution of walks that cross neighbour reproductions of the ℓth stage carpet in the next stage, leading to the true critical behaviour of DSAWs.

Our estimates of $\nu_\perp$ for both models on carpet 1 differ from the results obtained by Monte Carlo simulations on finite stages of that lattice [11, 12], probably due to finite size effects in the simulations. However, the trend $\nu_\perp > 0.5$ obtained in these simulations is also observed here for most lattices, specially for the high-lacunar ones. Also, our results show that PDSAW and FDSAW models belong to different universality classes for each carpet, in contrast to those results.

In conclusion, this work presents new results for the critical behaviour of DSAWs on Sierpinski carpets. The attainment of accurate estimates of critical exponents from series analysis open new perspectives for the quantitative study of universality classes of DSAWs on carpets and on other families of regular fractals.

Acknowledgment

We would like to thank F A da Costa Chalub for suggesting to us the use of the root method.

References

[1] Kinzel W 1993 *Percolation Structures and Processes* ed G Deutscher, R Zallen and J Adler (Bristol: Hilger)
[2] Nadal J P, Derrida B and Vannimenus J 1982 *J. Physique* **43** 1561
[3] Redner S and Majid I 1983 *J. Phys. A: Math. Gen.* **16** L307
[4] Szpilka A M 1983 *J. Phys. A: Math. Gen.* **16** 2883
[5] Blöte H W J and Hilhorst H J 1983 *J. Phys. A: Math. Gen.* **16** 3687
[6] Cardy J L 1983 *J. Phys. A: Math. Gen.* **16** L355
[7] Zhang Z Q, Yang Y S and Yang Z R 1984 *J. Phys. A: Math. Gen.* **17** 245
[8] Elezović-Hadžić S and Milošević S 1989 *Phys. Lett.* **138A** 481
[9] Elezović-Hadžić S, Milošević S, Capel H W and Post T 1991 *Physica* **179A** 39
[10] Mandelbrot B B 1982 *The Fractal Geometry of Nature* (San Francisco, CA: Freeman)
[11] Yao K-L and Zhang G-C 1990 *J. Phys. A: Math. Gen.* **23** L1259
[12] Yao K-L, Zhang G-C and Wang J-F 1991 *Commun. Theor. Phys. (China)* **16** 355
[13] Kim M H, Lee J, Park H and Kim I-M 1992 *J. Phys. A: Math. Gen.* **25** L453
[14] Aarão Reis F D A and Riera R 1992 *Phys. Rev.* A **45** 2628
[15] Aarão Reis F D A and Riera R 1993 *J. Stat. Phys.* **71** 453
[16] Aarão Reis F D A and Riera R 1994 *Phys. Rev.* E at press
[17] Aarão Reis F D A and Riera R 1994 *Physica* A at press
[18] Gaunt D S and Guttmann A J 1974 *Phase Transitions and Critical Phenomena* vol 3, ed C Domb and M S Green (London: Academic)
Guttman A J 1987 *J. Phys. A: Math. Gen.* **20** 1839
[19] Rehr J J, Joyce G S and Guttmann A J 1980 *J. Phys. A: Math. Gen.* **13** 1587
[20] Baker G A 1975 *Essentials of Padé Approximants* (New York: Academic)
[21] Havlin S and Ben-Avraham D 1987 *Adv. Phys.* **36** 695